H/F substituted perovskite compounds with above-room-temperature ferroelasticity: $[(CH_3)_4P][Cd(SCN)_3]$ and $[(CH_3)_3PCH_2F][Cd(SCN)_3]$

Ying-Jie Cao, Lin Zhou, Ping-Ping Shi, Qiong Ye* and Da-Wei Fu*

Syntheses

All used experimental reagents were of analytical grade without any further purification. Tetramethylphosphonium chloride was commercially available. The synthesis method of fluoromethyl-trimethyl-phosphonium bromine ($Me_3PCH_2F\cdot Br$): dehydrated acetonitrile (50 mL) was added into a dry flask under nitrogen at 0°C. Trimethylphosphine (4 mL, 40 mmol) was added to this solution via a syringe firstly. Then fluorobromomethane (3 mL, 47 mmol) pre-cooled to 0°C was dropped into the solution in an ice bath. The mixed solution was heated to 40°C and stirred for 5 h. Reaction mixture was cooled down to room temperature for about 10 min. Then the solvent was removed under vacuum, and the residue was dried to obtain $Me_3PCH_2F\cdot Br$ as a white solid. The mixture could be recrystallized from ethyl acetate and ethanol with a yield of about 60% based on trimethylphosphine. The product was stable except deliquescent, so the recrystallized product was quickly transferred to a reagent bottle and sealed after processing. **^{1}H NMR** (DMSO): δ 5.44-5.52 (dd, H), δ 3.34 (s, 1.25H), δ 2.50 (s, 1.89H), δ1.95-1.98 (d, 4.49H). **^{13}C NMR** (DMSO): δ 78.07 (dd), δ 39.8 (m, 20.61 C), δ 4.88 (d, 3.27 C). **^{19}F NMR** (DMSO): δ -173.12 (s). **^{31}P NMR** (DMSO): δ 27.73 (m) (Figure S8). The mass spectrum confirmed the phase purity of $Me_3PCH_2F^+$ (Figure S9).

Synthesis of **1** and **2**: Colourless strip crystals of $[(CH_3)_4P][Cd(SCN)_3]$ (**1**) and $[Me_3PCH_2F][Cd(SCN)_3]$ (**2**) were obtained by slowly evaporating aqueous solutions (about 60 mL) containing cadmium nitrate tetrahydrate (0.02 mol), sodium rhodanate (0.06 mol) and tetramethylphosphonium chloride (0.02 mol for **1**), $Me_3PCH_2F\cdot Br$ (0.02 mol for **2**), at room temperature for few days respectively. Compound **1** and **2** was verified by IR spectroscopy using a Shimadzu model IR-60 spectrometer (Figure S1) and PXRD patterns, which confirmed the phase purity of **1** and **2** (Figure S2).The peak at 2900-3000 cm^{-1} is attributed to the stretching vibration of C-H, the peak at 1300-1400 cm^{-1} is attributed to in-plane bending vibration peak of C-H and the peak at 650-1000 cm^{-1} may be due to out-plane bending vibration peak of C-H. The peak near 2000 cm^{-1} is the characteristic peak of C≡N. The infrared characteristic peak of the C−F bond from organic cation is located at about 1050 cm^{-1}.

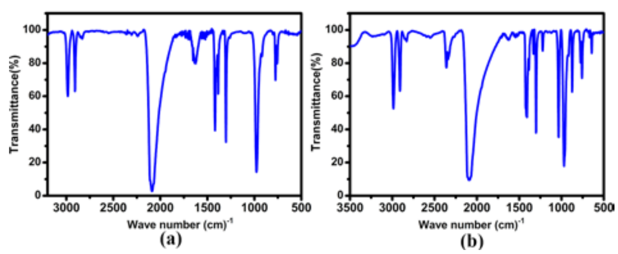

Fig. S1 IR spectrums of **1** (a) and **2** (b) measured on a KBr-diluted pellet at room temperature.

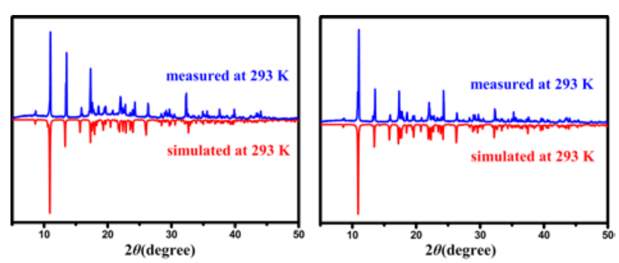

Fig. S2 Powder XRD patterns of **1** and **2** at 293 K.

Single-Crystal X-ray Crystallography

Data of variable-temperature X-ray diffraction of compound **1** and **2** was collected on a Rigaku Saturn 724 diffractometer with Mo Kα radiation (λ = 0.71073 Å) at different temperatures (293 K, 338 K or 333 K). The Crystal-Clear software package (Rigaku, 2005) was used to perform data reduction and multiscan absorption correction. Crystal structures were solved with direct method, and then refined by the SHELXLTL software package (SHELX-14) using full-matrix least-squares refinements on F^2. Non-hydrogen atoms were refined anisotropically with all H atoms being placed at ideal positions. The molecular structures and the packing views were drawn with DIAMOND (Brandenburg and Putz, 2005). Crystal data and structure refinement for **1** and **2** are given in Table S1.

Powder X-ray Diffraction

For compounds **1** and **2**, powder X-ray diffraction (PXRD) measurements on a PANalytical X'Pert PRO X-ray diffractometer were performed at 293 K. Diffraction patterns were recorded in the 2ϑ range 5–50° with a step size of 0.02°.

Thermal Measurements

The differential scanning calorimetry (DSC) data of **1** and **2** was recorded on a PerkinElmer Diamond DSC instrument at 10 K min^{-1} by heating/cooling under a nitrogen atmosphere in aluminum crucibles. The samples (6.7 mg for **1** and 7.2 mg for **2**) were placed in aluminium crucible at atmosphere.

Dielectric Constant Measurements

Crystalline powdered samples of **1** and **2** deposited with carbon conductive glue painted on both sides was used in dielectric studies. The complex dielectric permittivity ε ($\varepsilon = \varepsilon' - i\varepsilon''$, where ε´ and ε" are the real part and imaginary part, respectively) was measured on an impedance analyzer (TH2828A) in the frequency range from 50 kHz to 1 MHz, with an applied ac voltage at 1 V.

Optical measurements

Aqueous saturated solutions(100μL) of **1** and **2** were dropped onto a prepared indium tin oxide (ITO)-coated glass respectively, and thin films were obtained by the situ growth on a hotplate (Linkam THMSE 600 cooling/heating stage) at 343 K for 10 min. Optical observations were carried out by using an Eclipse E600 POL polarizing microscope (Nikon) equipped.

Table S1. Crystal data, data collection and reduction parameter of crystals of **1** and **2**.

	293K	338K	293K	333K
Chemical Formula	$C_7H_{12}CdS_3PN_3$		$C_7H_{11}CdFN_3PS_3$	
Formula weight	377.76		395.74	
Crystal system	Monoclinic	Orthorhombic	Monoclinic	Orthorhombic
Space group	*P*2$_1$/*c*	*Pmcn*	*P*2$_1$/*c*	*Pmcn*
a, Å	10.287(2)	10.2216(5)	10.3715 (3)	10.3487 (4)
b, Å	13.299(3)	13.3718(7)	13.1559 (4)	13.2129 (4)
c, Å	10.788(2)	10.6974(5)	10.7808 (3)	10.7451 (4)
α, deg	90	90	90	90
β, deg	95.07(3)	90	97.025 (3)	90
γ, deg	90	90	90	90
V, $Å^3$	1470.1(5)	1462.13(13)	1459.96 (7)	1469.25 (9)
Z	4	4	4	4
F(000)	744.0	744.0	776	772
Radiation (Mo Kα)	0.71073	0.71073	0.71073	0.71073
2Θ range for data collection, °	3.0–27.5	3.6-29.1	3.0-31.7	2.5-27.5
Reflections measured	10056	8781	11960	9907
Reflections independent	3333	1962	3809	2150
Reflections used	2116	1528	3241	1675
μ, mm^{-1}	2	2	2.02	2.01
Goodness-of-fit on F^2	1.06	1.07	1.083	1.01
Final R indexes [I>=2σ (I)]	R_1=0.080, wR_2=0.247	R_1=0.080, wR_2=0.271	R_1=0.072, wR_2=0.027	R_1=0.105, wR_2=0.462

Table S2. The key bond distances and angles of **1** at 293 K and 338 K

	N1—Cd1	2.315 (9)	N2—Cd1	2.439 (10)
	N3—Cd1	2.327 (10)	Cd1—S3	2.700 (3)
	Cd1—S1	2.768 (3)	Cd1—S2	2.726 (3)
293K	N3—C3—S2^{i}	177.9 (11)	N1^{i}—C1—S1	178.2 (11)
	N2^{ii}—C2—S3	170.5 (11)	C3^{ii}—S2—Cd1	97.5 (4)
	C2—S3—Cd1	101.5 (4)	C1—S1—Cd1	95.9 (3)

	C2^{i}—N2—Cd1	132.0 (10)	C1^{ii}—N1—Cd1	154.0 (8)
	C3—N3—Cd1	149.6 (9)		

Symmetry codes: (i) *x*, −*y*+1/2, *z*+1/2; (ii) *x*, −*y*+1/2, *z*−1/2.

338 K	N1—Cd1	2.319 (10)	S2—Cd1	2.713 (3)
	Cd1—S1	2.762 (3)	Cd1—N2^{iii}	2.378 (9)
	N2—Cd1	2.378 (9)	Cd1—S2^{iii}	2.713 (3)
	N2—C2—S2^{i}	174.5 (9)	N1^{ii}—C1—S1	178.2 (9)
	C2—N2—Cd1	140.2 (10)	C1^{iii}—N1—Cd1	152.7 (8)
	C2^{iv}—S2—Cd1	99.1 (3)	C1—S1—Cd1	95.2 (4)

Symmetry codes: (i) *x*, −*y*+1/2, *z*+1/2; (ii) −*x*+1/2, −*y*+1/2, *z*+1/2; (iii) −*x*+1/2, *y*, z.

Table S3. The key bond distances and angles of **2** at 293 K and 333 K

293K	Cd1—N2^{i}	2.293 (6)	Cd1—S1	2.7195 (19)
	Cd1—N1	2.343 (7)	Cd1—S3	2.7363 (19)
	Cd1—N3	2.424 (7)	Cd1—S2	2.713 (2)
	N3—C6—S1^{ii}	171.3 (7)	N1^{i}—C7—S2	178.1 (7)
	N2—C5—S3	179.6 (7)	C5—S3—Cd1	96.3 (2)
	C6^{i}—S1—Cd1	102.5 (2)	C7—S2—Cd1	98.0 (2)
	C6—N3—Cd1	131.1 (7)	C5—N2—Cd1^{ii}	154.5 (5)
	C7^{ii}—N1—Cd1	149.9 (6)		

Symmetry codes: (i) *x*, −*y*+1/2, *z*−1/2; (ii) *x*, −*y*+1/2, *z*+1/2.

333K	Cd1—N1	2.291 (4)	Cd1—S1^{i}	2.7346 (13)
	Cd1—N2^{i}	2.362 (5)	Cd1—S1	2.7346 (13)
	Cd1—N2	2.362 (5)	Cd1—S2	2.7414 (13)
	N1—C5—S2^{ii}	179.5 (4)	N2—C4—S1^{iii}	175.5 (4)
	C5^{ii}—S2—Cd1	96.39 (16)	C4^{iii}—S1—Cd1	99.55 (15)
	C5—N1—Cd1	154.7 (4)	C4—N2—Cd1	139.1 (4)

Symmetry codes: (i) −*x*+1/2, *y*, *z*; (ii) −*x*+1/2, −*y*+1/2, *z*−1/2; (iii) *x*, −*y*+1/2, *z*+1/2.

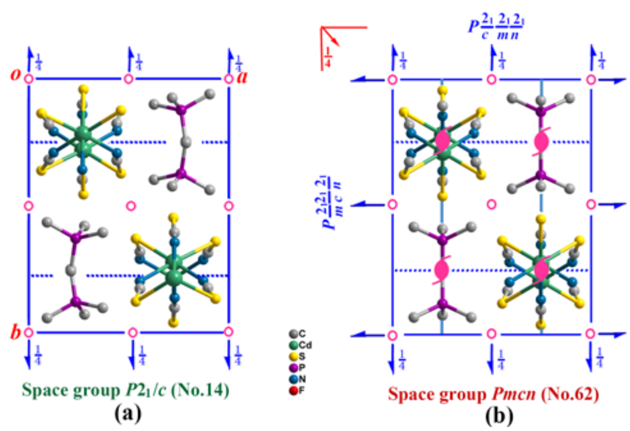

Fig. S3 The unit cell packing and spatially symmetric operations change of **1** from RTP (a) to HTP (b)

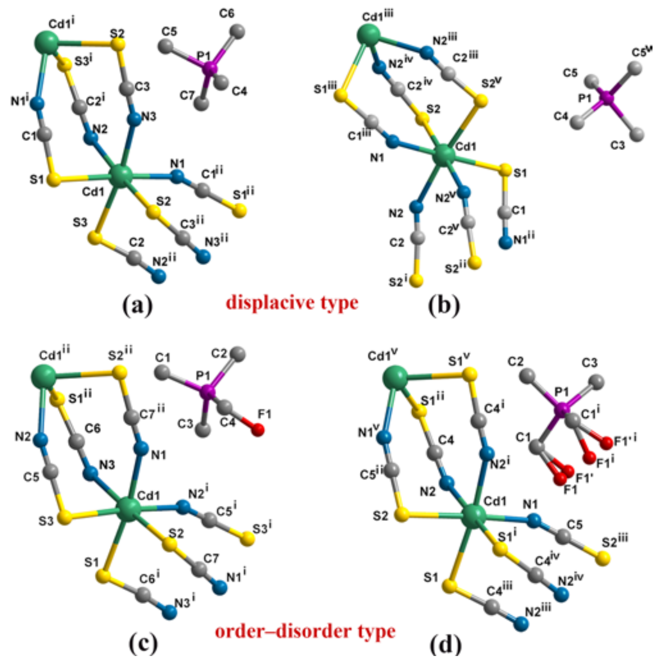

Fig. S4 Molecular structures of **1** shown at (a) 293 K and (b) 338 K and of **2** shown at (c) 293 K and (d) 333 K. All H atoms omitted for clarity. [Symmetry codes: (i) *x*, −*y*+1/2, *z*+1/2; (ii) *x*, −*y*+1/2, *z*−1/2. (b) (i) *x*, −*y*+1/2, *z*+1/2; (ii) −*x*+1/2, −*y*+1/2, *z*+1/2; (iii) −*x*+1/2, −*y*+1/2, *z*−1/2; (iv) *x*, −*y*+1/2, *z*−1/2; (v) −*x*+1/2, *y*, *z*. (c) (i) *x*, −*y*+1/2, *z*−1/2; (ii) *x*, −*y*+1/2, *z*+1/2. (d) (i) −*x*+1/2, *y*, *z*; (ii) −*x*+1/2, −*y*+1/2, *z*+1/2; (iii) *x*, −*y*+1/2, *z*−1/2; (iv) −*x*+1/2, −*y*+1/2, *z*−1/2; (v) *x*, −*y*+1/2, *z*+1/2.]

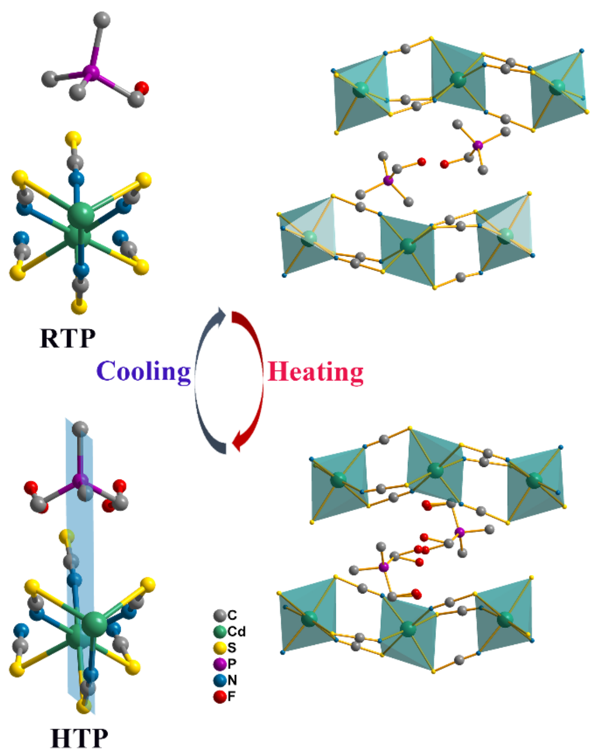

Fig. S5 Structures of **2** in the HTP (293 K) and HTP (333 K).

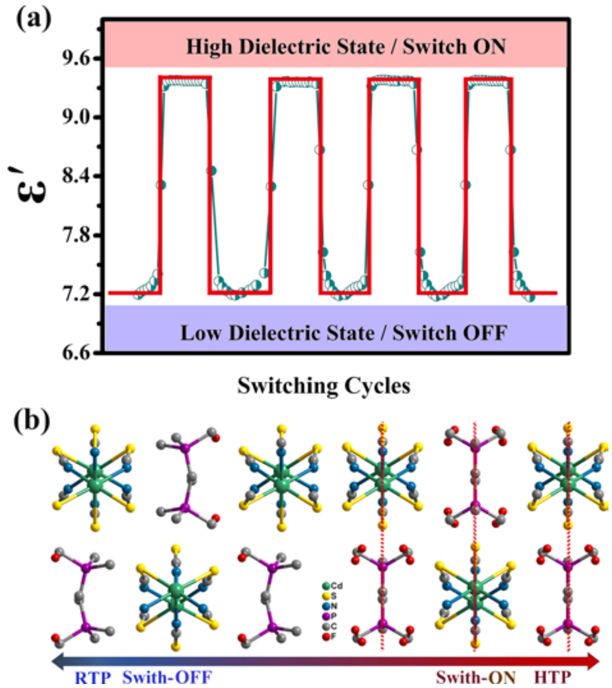

Fig. S6 (a) The recoverable switching dielectric effects of **2** at 1 MHz. (b) Schematic diagram for the generation of molecular structure change in **2** during the switching process (red dotted line indicates mirror)

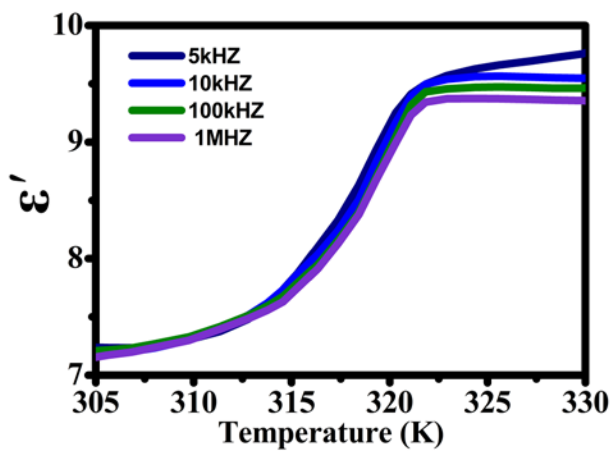

Fig. S7 The ε′ of **2** at frequencies from 5 kHz to 1000 kHz upon cooling.

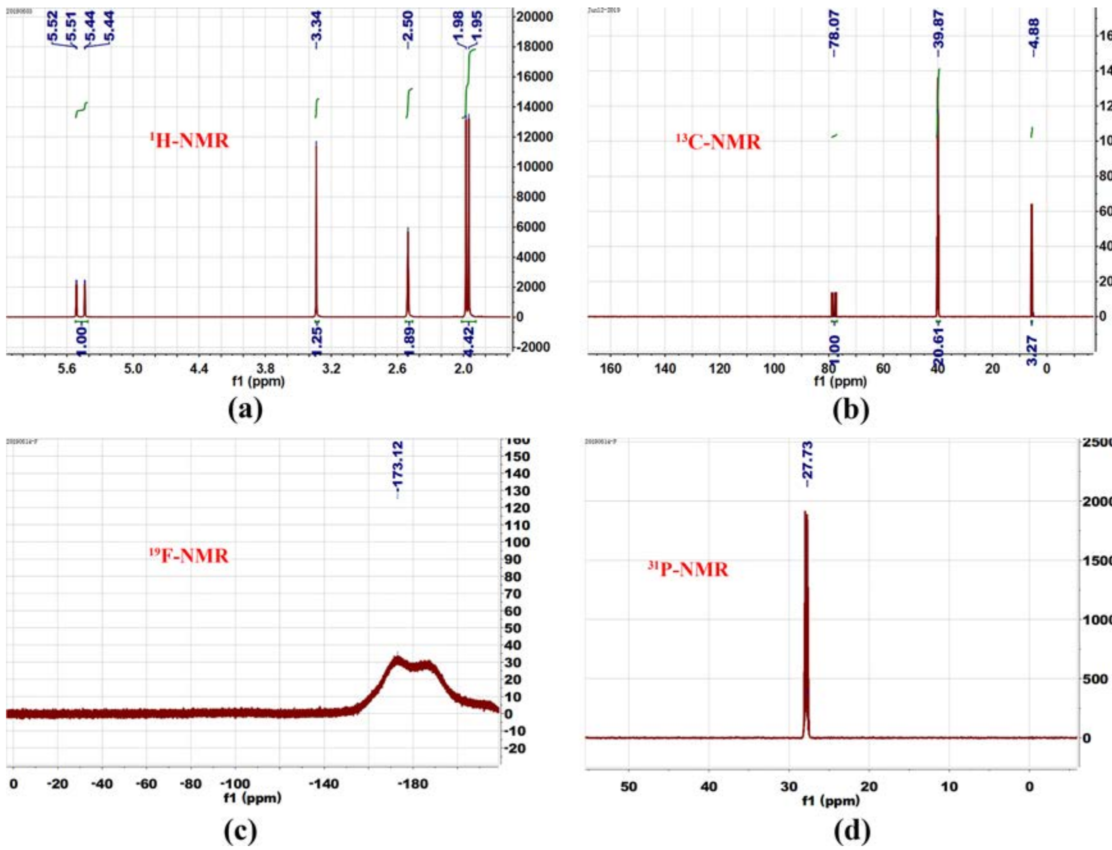

Fig. S8 The ^{1}H(a),^{13}C(b), ^{19}F(c) and ^{31}P(d) NMR of $Me_3PCH_2F\cdot Br$

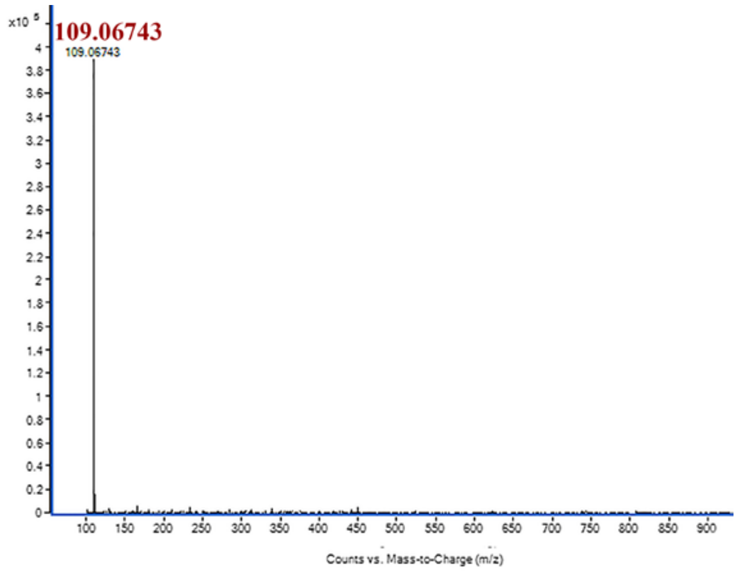

Fig. S9 The mass spectrum of $Me_3PCH_2F^{+}$